DEVELOPMENT OF AN ADVANCED NO-MOVING-PARTS HIGH-LIFT AIRFOIL

Robert J. Englar*, CCW Program Manager, Aircraft Division
David Taylor Naval Ship Research and Development Center
Bethesda, Maryland 20084

Abstract

An advanced Circulation Control Wing (CCW) airfoil has been developed by incorporating a very small radius blown trailing edge into the aft profile of an existing supercritical airfoil. This combined no-moving-parts configuration generates the same high lift as the already flight-proven large-radius CCW airfoils (section lift coefficient near 7), yet produces negligible unblown drag penalty due to leaving the device deployed for cruise flight. The large leading edge radius of the supercritical airfoil allows high-lift operation without mechanical deflection. Experimental results presented by the paper imply the feasibility of an efficient mono-element cruise and high-lift airfoil, with transition between the two modes accomplished by merely initiating blowing from the fixed trailing edge slot. Comparisons to existing blown and unblown high lift systems are made, and possible applications are discussed.

Introduction

The Circulation Control Wing (CCW) concept has recently been proven both experimentally and in flight demonstrations as a very effective yet mechanically simple blown high-lift system capable of significant short takeoff and landing (STOL) characteristics and heavy lift potential.[1-4] As applied to a typical fixed-wing aircraft, the concept employs engine bleed air blown tangentially over a rounded trailing edge to amplify the airfoil circulation and thus its high lift capability. Figure 1 shows a typical application of CCW to the existing airfoil section of the Grumman A-6 aircraft. [1,3] During the development of this concept into the A-6/CCW flight demonstrator configuration, wind-tunnel evaluation [1] of this two-dimensional model with CCW installed showed more than a tripling of the maximum lift coefficient of the conventional airfoil with a 60-degree flap deflection. Figure 2 shows this increased lifting capability of CCW. The configurations and geometries developed in these investigations were incorporated in the flight demonstrator A-6/CCW of Figure 3. The effectiveness of the round CCW trailing edge in turning flow around the airfoil in flight resulted in very strong lift augmentation at the lower blowing rates obtainable from existing engine bleed, and in the significant STOL performance and heavy lift potential [1,2,5,6] shown in Figure 4.

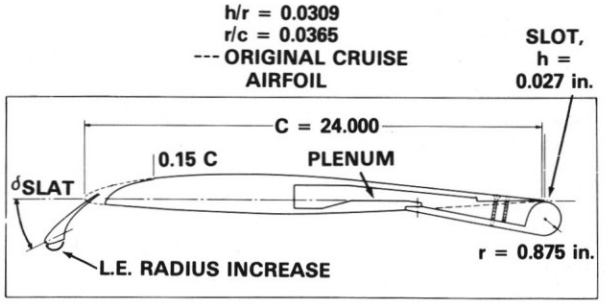

Fig. 1 - A-6/CCW Wing-Fold Airfoil Section (64A008.4/CCW)

These flight results confirmed the CCW as a simple and effective blown STOL system, and also identified several improvements necessary before the system could be incorporated on production aircraft. The A-6/CCW flight demonstrator airfoil incorporated a state-of-the-art large trailing edge radius of 3.67 percent chord to guarantee a successful flight demonstration, but any operational use of this design would require mechanized retraction of this system into the wing to avoid the cruise drag penalty. An alternative for minimizing this drag problem is to reduce the trailing edge size to the point where it incurs no base drag penalty relative to the conventional airfoil. A second problem area was the mechanized leading edge device required to prevent flow separation at the

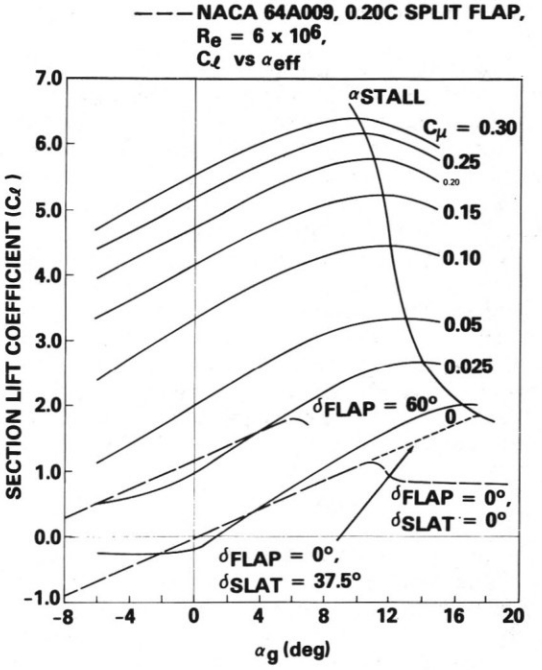

Fig. 2 - Lift Characteristics of the NACA 64A008.4/CCW Airfoil

Fig. 3 - A-6/CCW Flight Demonstrator Aircraft

*Member of AIAA

BASED ON FLIGHT DEMONSTRATION RESULTS TOGW = 35,700 LB., LGW = 33,000 LB. CORRECTED TO SEA LEVEL, STANDARD DAY	A-6 (30° FLAPS)	A-6/CCW
85% INCREASE IN $C_{L_{MAX}}$	2.1	3.9 ($C_\mu = 0.30$)
35% REDUCTION IN POWER-ON APPROACH SPEED	118 KTS ($C_L = 1.49$)	76 KTS (0.75 P_{MAX}, $C_\mu = 0.14$, $C_L = 2.78$)
65% REDUCTION IN LANDING GROUND ROLL	2450 FT	900 FT
30% REDUCTION IN LIFT OFF SPEED	120 KTS ($C_L = 1.41$)	82 KTS (0.6 P_{MAX}, $C_\mu = 0.04$, $C_L = 2.16$)
60% REDUCTION IN TAKEOFF GROUND ROLL	1450 FT	600 FT
75% INCREASE IN PAYLOAD/FUEL AT TYPICAL OPERATING WEIGHT (EW = 28,000 LB.)	45,000 LB.	58,000 LB.

Fig. 4 - A-6/CCW STOL Performance Summary

high circulation associated with STOL operation. On the flight demonstrator, the existing 25 degree deflection of the leading edge slat was insufficient to assure flow attachment, and an increased leading edge radius had to be added. This was satisfactory on the demonstrator, but would also have to be mechanically retracted to convert to the cruise airfoil.

In order to address the above areas, a program was undertaken to develop an advanced CCW airfoil which would incorporate a small round trailing edge, a blowing plenum, and a non-deflecting leading edge device all within the contour of the existing cruise airfoil. This would provide the potential for a no-moving-parts high-lift system which would not have to be retracted for cruise, the conversion between the two modes being merely the termination or initiation of blowing. Ideally, this combination single-element CCW airfoil would experience only a minimal lift loss relative to the larger trailing edge CCW configurations, and a negligible drag penalty in cruise relative to conventional sharper trailing edge airfoils. The following sections will discuss the design considerations and experimental evaluations involved in the development of the desired airfoil, and compare its performance to the desired goals.

Design Considerations

The above goals appeared to be obtainable by taking advantage of the large leading and trailing edge thickness of a typical bluff trailing edge supercritical airfoil. Not only does this airfoil section geometry appear quite compatible with the incorporation of aft plenum, slot and small radius trailing edge, it also generates the excellent transonic cruise performance afforded by increased critical Mach number and delayed drag rise. The development approach taken was to combine a typical proven supercritical section with a set of baseline CCW trailing edge parameters closely matching those of the A-6/CCW aircraft, and then experimentally evaluate the characteristics produced by progressively reducing the trailing edge size until it was most compatible with the supercritical air-

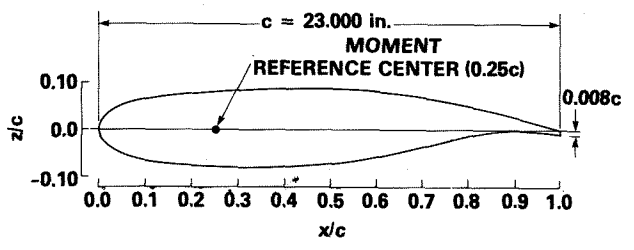

Fig. 5 - NASA 17-Percent-Thick Supercritical Airfoil Section (from Reference 7)

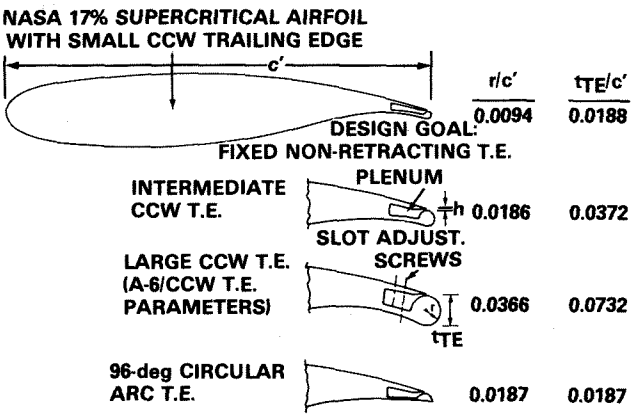

Fig. 6 - CCW/Supercritical Airfoil Model Geometries

foil aft contour. The NASA 17-percent-thick supercritical airfoil shown in Figure 5 had been both wind-tunnel tested [7,8] and flight tested [7,9], and therefore had a suitable reference data base. The airfoil thickness produces a large bluff leading edge radius of 4.28-percent chord, which is of such substantial size that the radius could substitute for a mechanical leading edge device and thus further simplify the high-lift configuration. To parametrically vary the model trailing edge geometry, the A-6/CCW design radius-to-chord ratio of 0.0367 was taken as a baseline reference value, halved to give $r/c' = 0.0188$ and halved again to give $r/c' = 0.0094$. These will be referred to as the large, intermediate, and small trailing edges in the following discussions. The smallest trailing edge diameter (0.0188c') is thus slightly greater than twice the 0.008c trailing edge thickness of the baseline supercritical airfoil. These model configurations are shown in Figure 6, where the pertinent CCW trailing edge parameters are also identified. The terms r, h, c and c' represent trailing edge radius, jet slot height, original baseline airfoil chordlength, and effective airfoil chordlength, respectively.

Of primary importance in these investigations is the effect of variation in trailing edge slot-height-to-radius ratio (h/r) and radius-to-chord ratio (r/c'). Because Reference 4 suggests that strongly attached Coanda flow is maintained for $0.01 \leq h/r \leq 0.05$, and effective jet turning and lift augmentation result from $0.02 \leq r/c' \leq 0.05$, the reduced radius configurations may exceed these guidelines. The effects of this will be an important test result.

An alternate trailing edge, shown at the bottom of Figure 6, was designed in case the small radius proved unable to yield large lift augmentation. By employing twice the radius but a smaller portion of circular arc, the 0.0187c' design thickness and tendency for attached flow are maintained, but jet turning is limited to the 96-deg arc which ends at the sharp trailing edge. Lift augmentation will thus be limited by the maximum flow turning of 96 deg.

Experimental Apparatus and Technique

The 3-ft span two-dimensional models described above were mounted between the 3- by 8-ft subsonic two-dimensional wall inserts installed in the DTNSRDC 8- by 10-ft subsonic tunnel. Lift and moment coefficients were obtained by numerical integration of surface static pressures near the midspan as recorded by a 144-port scanivalve system. The drag coefficient was obtained from integration of wake momentum deficit as measured on a fixed total head wake

rake spanning nearly 8 ft from floor to ceiling. All reported force and moment coefficients are based on c', since this is considered to be the undeflected cruise reference chord. The momentum coefficient C_μ was calculated as $\dot{m}V_j/(qc')$, where $\dot{m}$ is the mass flow per unit slot span as measured by venturimeter, and V_j is the isentropic jet velocity calculated using the equation in Reference 4. Model installation, test apparatus and technique, data reduction and corrections, and monitoring of tunnel two-dimensionality were all conducted as reported in Reference 4 (Appendix A) and Reference 8.

Results and Discussion

Experimental investigations were conducted on the Figure 6 configurations, where blowing pressure and then slot height were varied for each configuration at a geometric incidence of 0 deg. Additional variations were made in Reynolds number and angle of attack before conversion to the next trailing edge configuration. The following discussion concentrates mainly on the effects of these variables and the resulting performance of the four trailing edge geometries.

Lift Augmentation due to Blowing

Section lift coefficient C_ℓ is presented in Figure 2 as a function of momentum coefficient and incidence for the A-6/CCW airfoil section to allow comparisons of the lift performance of the CCW/Supercritical airfoils with that of a state-of-the-art CCW airfoil. Figure 1 shows the relative size of the rounded trailing edge and emphasizes the need to reduce that geometry to the smaller trailing edges of Figure 6. For the large and small CCW trailing edge configurations applied to the supercritical airfoil, section lift coefficients are presented in Figure 7 and 8 as functions of momentum coefficient and slot height at 0-deg incidence and nominal free-stream dynamic pressure of 10 psf. An increase in slot height yielded increased lift at constant C_μ until some upper limit on slot height or C_μ was reached. For the large CCW configuration, the largest slot height caused reductions in lift for all values of C_μ; but for the small radius trailing edge, larger slot heights produced larger lift until a certain value of C_μ was reached, after which lift dropped significantly. This was found to be a function of the effect of pressure ratio on the degree of blowing jet attachment which could be sustained by the small radius. (See Reference 10 for a discussion of jet detachment at higher pressures for small radii.) In Figure 9, it is confirmed that for each slot height, a blowing pressure ratio, (P_D/P_∞) exists beyond which lift reduces with increased blowing on the small radius airfoil. The Figure 9 data emphasize the effectiveness of the small trailing edge airfoil when run at the low pressure ratios (and corresponding higher slot heights) characteristic of powering the airfoil with turbofan engine bypass airflow, where pressure ratios of about 1.5 are typical.

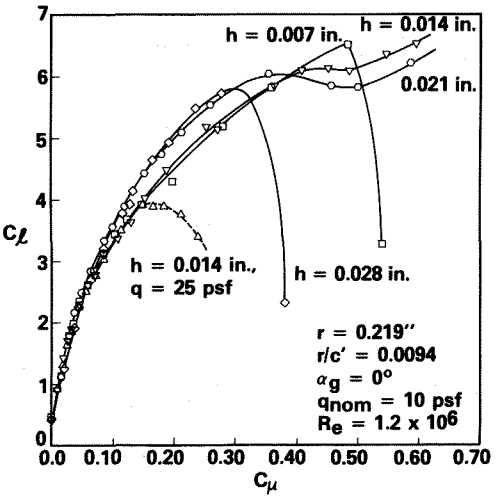

Fig. 8 - Lift Augmentation for the Small Trailing Edge CCW/Supercritical Airfoil

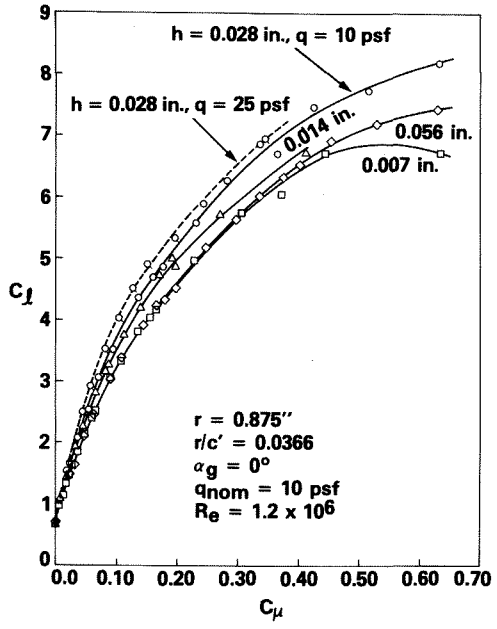

Fig. 7 - Lift Augmentation for the Large Trailing Edge CCW/Supercritical Airfoil

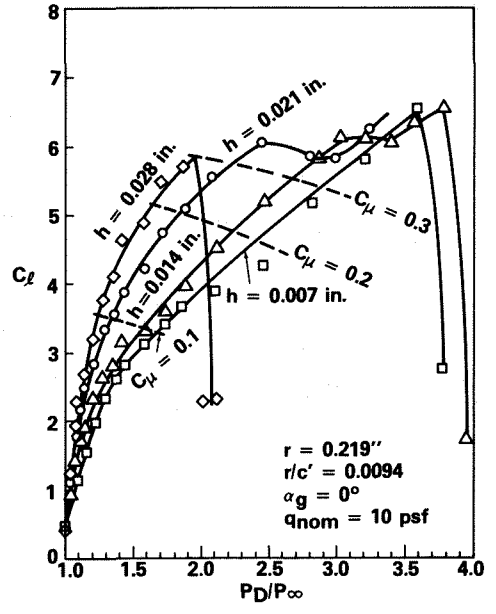

Fig. 9 - Lift as a Function of Blowing Pressure Ratio for the Small Trailing Edge Airfoil

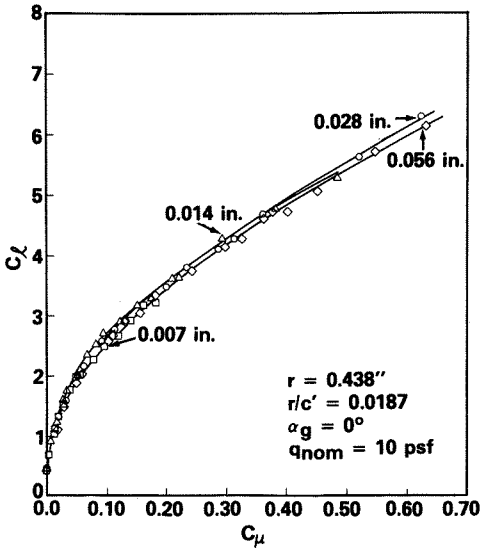

Fig. 10 - Lift Augmentation for the 96-degree Circular Arc Trailing Edge.

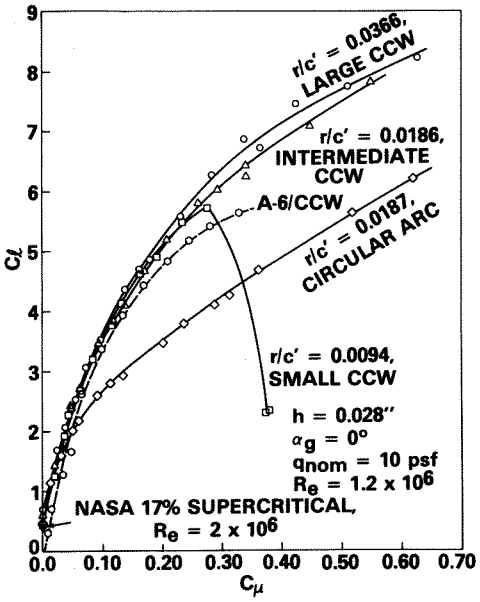

Fig. 11 - Comparative Lift Performance of CCW Airfoils

Figure 10 offers an alternative to the small completely round trailing edge at higher C_μ: the circular arc trailing edge which ends in a sharp corner at approximately 96 deg from the slot. This fixes the jet separation point and minimizes the effects of slot height change. It also produces less lift than the full round configurations, but seems to assure jet attachment at much higher pressure ratios and C_μ values. The performance of this airfoil closely resembles the characteristic jet flap thrust recovery, to be discussed in a later section.

Comparative Lift Performance

In Figure 11, the four supercritical airfoil configurations are compared with each other at the same slot height, Reynolds number, and incidence, and to the A-6/CCW airfoil at a similar slot height but a higher Reynolds number (1.9 x 10^6, q = 25 psf). For $C_\mu < 0.26$, reduction in trailing edge radius on the CCW/Supercritical airfoil produces only a slight change in C_ℓ. At a typical C_μ of 0.25, the small radius configuration generates only 5 percent less lift than the same configuration with a radius four times as large. In Figure 12, for h = 0.014 in. the reduction in lift is 7 percent, but the lift dropoffs in the small radius data occur at much higher C_μ. All three round trailing edges perform better than the A-6/CCW airfoil at α_g = 0 deg, probably because of the slat download and the resulting lift loss. The basic 17-percent supercritical airfoil without blowing [7] generates only C_ℓ = 0.4 at this incidence. The 96-deg circular arc airfoil generates less circulation lift than the other round trailing edges due to the fixed jet separation point locations and limited flow turning.

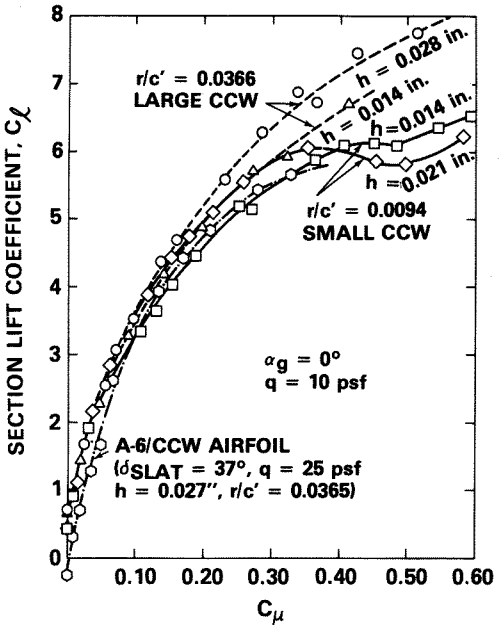

Fig. 12 - Comparative Lift Performance of the Large and Small Trailing Edge CCW Airfoils

Lift Variation with Incidence

The small radius CCW airfoil was evaluated over a geometric angle-of-attack range from -5 deg to +15 deg. These lift data for the 0.014 in. slot height are presented as functions of blowing and incidence in Figure 13. If these plots are compared to the state-of-the-art A-6/CCW airfoil data of Figure 2, which was run at a larger slot height and Reynolds number, two trends are noticeable. First, the CCW/Supercritical airfoil, with a radius only 25 percent as large, produces lift that is slightly greater than the A-6/CCW airfoil at lower α and C_μ, since the A-6 slat imparts a download under these conditions. Second, the undeflected bulbous nose of the supercritical airfoil provides the same or better leading edge performance as the A-6 model's 37.5 deg slat, yielding almost identical stall angles at any given C_ℓ.

The apparent deficits in certain of the lift curves (primarily for 6 deg $\leq \alpha_g \leq$ 12 deg and $C_\mu < 0.20$) are due to flow separation on the supercritical airfoil aft upper surface, between the crest and the slot. (This condition is discussed in Reference 11.) The separated flow is re-entrained at higher C_μ, and the deficits disappear. The same correction should occur at higher Reynolds numbers.

Drag due to Blowing and Incidence

Two-dimensional drag coefficients obtained from wake rake pressure integrations are presented in Figure 14 for the small CCW/Supercritical and the circular arc configurations at α_g = 0 deg. Initiation of blowing causes an immediate reduction in measured drag coefficient because, at these low jet turning conditions, the jet momentum is recovered as thrust and the wake momentum deficit is diminished. For the 96-deg circular arc, this trend of reducing drag by increasing C_μ continues throughout the entire range of blowing tested since the jet turning angle is fixed; however, for the full round trailing edge, the jet continues to turn as C_μ increases. As a result, thrust recovery diminishes, a larger viscous wake is generated, and drag begins to increase. This increase in drag is also due to the increased profile drag caused by large negative pressure regions over the round trailing edge, and thus larger drag values occur at higher blowing. The comparison between the circular arc and small radius CCW configuration, both of which have the same trailing edge thickness, shows lower drag for the former.

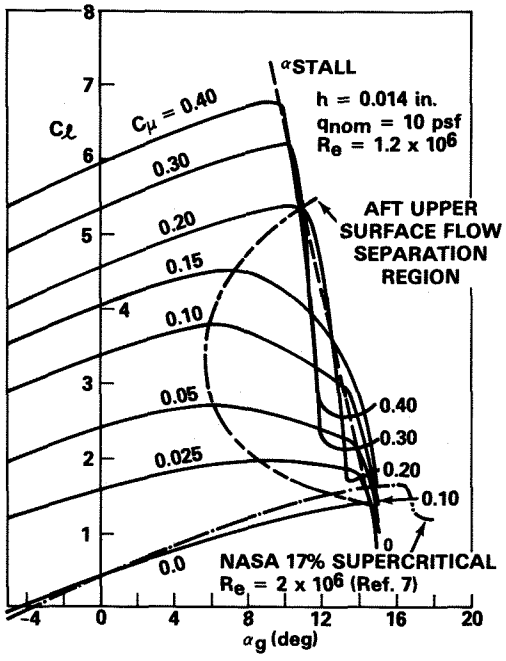

Fig. 13 - Variation in Lift with Incidence at Constant Blowing for the Small Trailing Edge CCW/Supercritical Airfoil

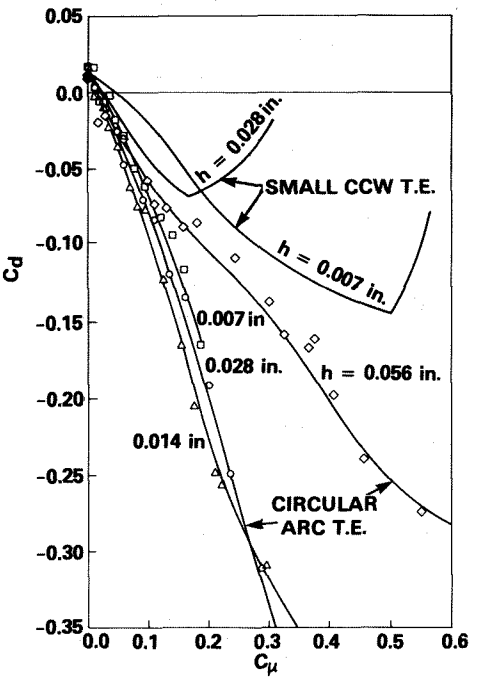

Fig. 14 - Variation in Drag Coefficient and Thrust Recovery with Blowing at α_g = 0°

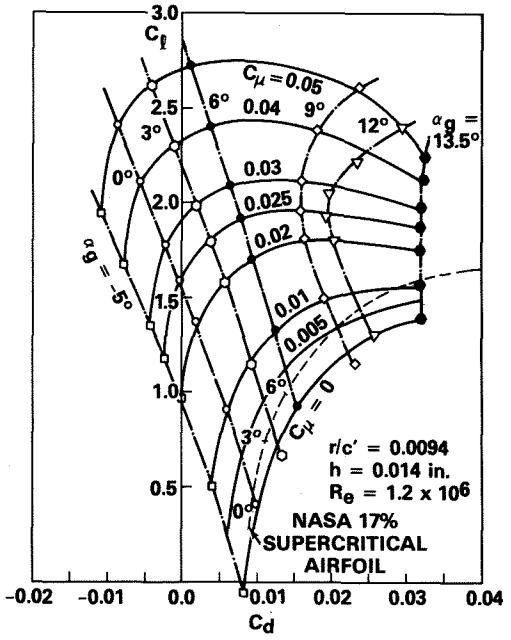

Fig. 15 - Drag Polars for the Small Trailing Edge CCW Airfoil at Low Blowing

Drag polars for the small radius airfoil at low blowing values are compared in Figure 15 with the baseline 17-percent supercritical airfoil. The drag values of the baseline airfoil are slightly lower than those of the CCW/Supercritical airfoil with no blowing (ΔC_d = 0.0006 at α_g = 0 deg); however, the drag of the CCW airfoil can be reduced to that of the baseline airfoil by blowing at $C_\mu \leq 0.005$ for $\alpha_g \leq 9$ deg. Additional blowing will reduce the drag even further, but an analysis of engine thrust loss due to required bleed needs to be considered. Thus, the high-lift device of the small CCW airfoil may be left exposed for cruise conditions with essentially no drag penalty.

This unblown drag reduction is further emphasized in Figure 16 as a function of Reynolds number. Drag coefficient reduces noticeably with Reynolds number for the large radius, but rather insignificantly for the small one. Once the transition value is reached and C_d becomes constant, the small trailing edge value is half of the large one. A sharp trailing edge NACA 64_3-418 airfoil[12] is included here for comparison, as is the baseline NASA supercritical airfoil.[7] At R_e = 2 x 10^6, the unblown lift and drag values at α_g = 0 deg are:

Airfoil	C_d	C_ℓ
64_3-418 (R_e = 3 x 10^6)	0.0061	0.330
Baseline supercritical	0.0084	0.400
Small CCW, r/c' = 0.0094	0.0090	0.455
Large CCW, r/c' = 0.0366	0.0183	0.671

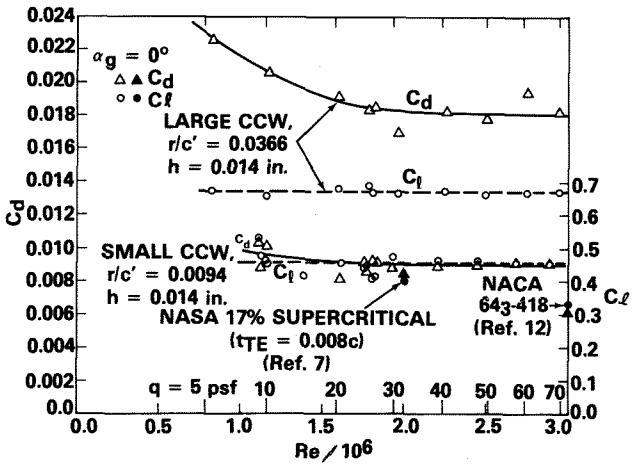

Fig. 16 - Unblown Lift and Drag Comparisons at α_g = 0°

Pitching Moment

As is typical of most blown airfoils, the increased suction region near the trailing edge blowing source generates increased nose-down pitching moment, as is verified in Figure 17 for the CCW airfoil sections. Increase in incidence adds leading edge suction regions which counteract those at the trailing edge and thus reduce the nose-down moment. Quarter-chord pitching moments at 0-deg incidence and q = 10 psf for the four supercritical configurations follow trends similar to those of the A-6/CCW airfoil; however, for most of the data shown, the supercritical configurations generate the same or less nose-down moment. At lift coefficients less than 5 there is little difference between the configurations. This nose-down pitch was trimmable with modification to the existing stabilizer on the A-6/CCW.[1-3] Longitudinal trim should thus be less a problem than on the A-6/CCW. With blowing on, the aircraft will be so stable longitudinally that its center of gravity may be moved further aft than the mean quarter chord, thus reducing the tail trim requirements.

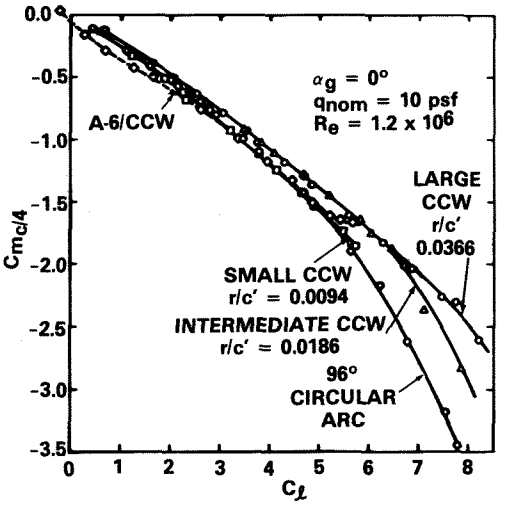

Fig. 17 - Comparative Quarter-Chord Pitching Moments of CCW Airfoils, h = 0.028 in.

Applications

The results above support a number of possible applications, both commercial and military, where the benefits of a single-element no-moving parts high-lift airfoil will allow aircraft designed to specific missions without compromising the wing to allow for takeoff and landing operations. Provisions for heavy lift and STOL capability without increased wing weight and complexity but with increased reliability could allow Naval operations from smaller air-capable ships, or Air Force operations from runways shortened by attack. The performance of the A-6/CCW demonstrator confirmed these CCW capabilities, which may now be obtained with considerable simplifications to the CCW airfoil. Figures 18-20 present a summary of lift results for the small trailing edge CCW/Supercritical airfoil and lift characteristics of several of the more effective high lift systems now in use on current aircraft or postulated for future designs. Note that the lifting capabilities are similar (maximum C_ℓ in the 5-8 range) but that mechanical complexity and/or blowing required vary significantly. Figure 19 shows a blown flap system [13] similar to those already in application on some military high performance aircraft where STOL performance offers a strong payoff (carrier operations, short field operation, etc). The needs for mechanical flap actuators and a leading edge device are evident, as is the requirement for a much higher blowing coefficient to achieve this lift level. These higher C_μ values are normally not available from conventional engine bleed. Figure 20 represents typically complex mechanical multi-element airfoils [14] such as those employed on current day commercial transports, where slats and triple-slotted mechanical flaps are

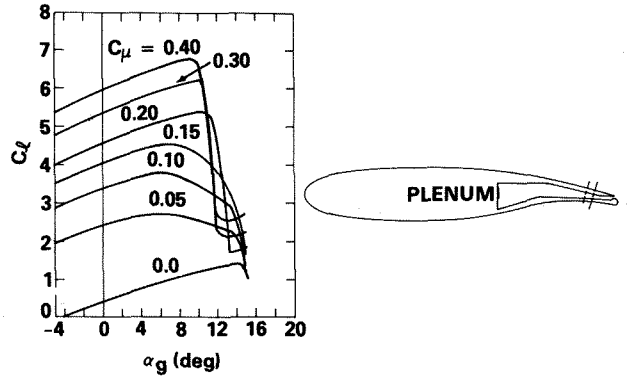

Fig. 18 - Lift Capabilities of the Small Trailing Edge CCW/Supercritical Airfoil

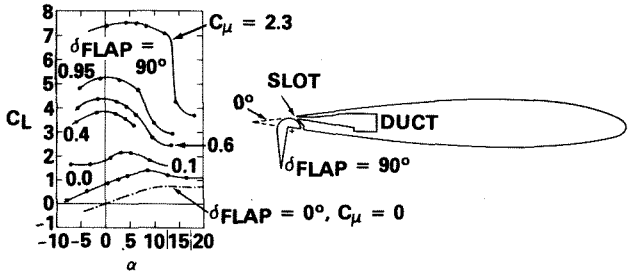

Fig. 19 - Lift Capabilities of a Tangentially Blown Flap (From Reference 13)

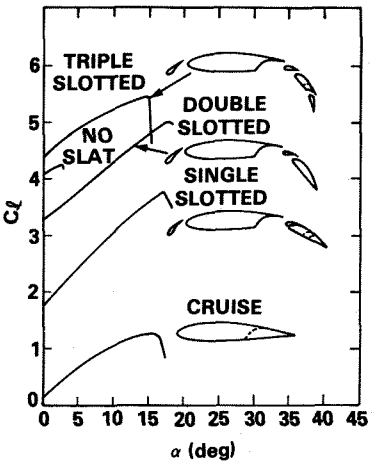

Fig. 20 - Multi-Element High-Lift Airfoils with Mechanical Flaps and Slats

required to achieve $C_\ell > 5$. This complexity is further compounded when the extended tracks, hinges and mechanical support brackets necessary to deploy these devices are considered. Comparison of these mechanisms to the simplicity of Figure 18 shows great promise for CCW application to commercial transports where supercritical airfoil sections are already being incorporated to improve transonic cruise performance.

In all the above comparisons, the main advantages of the CCW/Supercritical airfoil are mechanical simplicity and weight reduction due to lack of moving parts, and in the reduced amount of airflow required to achieve the high lift levels. An advanced CCW STOL aircraft[5,6,15] intended for Navy sea-based missions which could include airborne early warning, anti-submarine warfare, carrier onboard delivery, and fuel tanker, is shown in Figure 21. The outboard wing panel uses the CCW/Supercritical small radius airfoil for high lift generation powered by turbofan bypass air. The inboard section uses the strong flow entrainment property of CCW to deflect the thrust of the turbofan engines, mounted in an Upper Surface Blowing (USB) configuration. Variable thrust deflection achieved by trailing edge blowing pressure variation adds a vertical thrust contribution to lift without use of a mechanical flap. This combined CCW and USB system has already been confirmed experimentally[15] and offers a very simple effective STOL system for Navy aircraft.

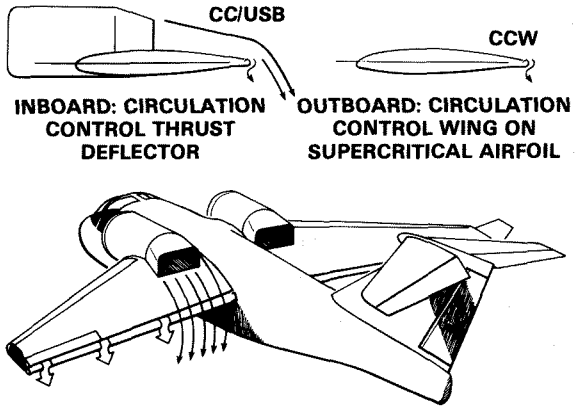

Fig. 21 - Proposed CCW + CC/USB STOL Aircraft

Conclusions and Recommendations

Circulation control wing technology was applied to a NASA 17-percent thick supercritical airfoil. Circular trailing edges of three different radii were evaluated: a large radius comparable to the A-6/CCW aircraft, a small radius approximately twice the thickness of the supercritical airfoil trailing edge, and an intermediate radius between these two. A fourth configuration was developed using 96 deg of circular arc with the intermediate size radius. The results of subsonic two-dimensional wind tunnel investigations indicate the small trailing edge size can be applied to a supercritical airfoil without degrading either high-lift or cruise performance. The following conclusions resulted from these investigations, and are summarized in Figure 22:

- All CCW/Supercritical configurations with full round trailing edges produced greater lift at $\alpha_g = 0$ deg than the A-6/CCW airfoil. At $C_\mu = 0.25$, the small CCW/Supercritical airfoil surpassed A-6/CCW airfoil lift by 3 percent and lift of the baseline supercritical cruise airfoil by 1250 percent.
- On the supercritical airfoil, reduction in trailing edge radius size from a state-of-the-art value (0.0366c') to 25 percent that size resulted in lift losses of only 5 to 7 percent at zero incidence, depending on C_μ and slot height. Lift coefficients greater than 6.5 were generated at $\alpha_g = 0$ deg for both configurations.
- Base drag was minimized by the small trailing edge radius so that unblown subsonic C_d was nearly the same as for the baseline 17-percent supercritical section. Drag could be further reduced on the small radius CCW airfoil to less than that of the baseline airfoil by minimal blowing.
- The large bulbous nondeflecting leading edge of the supercritical airfoil provided flow-attachment capability the same as or better than the A-6/CCW airfoil's 37.5-deg leading edge slat. A C_ℓ near 7 at $C_\mu = 0.4$ and $\alpha_g = 10$ deg was generated by the small radius CCW airfoil.
- The CCW/Supercritical small configuration produced increased C_ℓ at larger slot heights as long as certain pressure ratio limits were not exceeded. This makes it especially compatible with the low pressure, high mass flow characteristics of turbofan bypass airflow.
- Nose-down pitching moments for all supercritical blown configurations were equal to or less than those of the flight-trimmable A-6/CCW airfoil for $C_\mu \leq 0.25$.

These results suggest the strong potential of a combined cruise and high-lift mono-element airfoil, where the favorable characteristics of each airfoil are retained without compromising the other, and no mechanical moving parts are required to transition from one mode to the other. Negligible drag penalties occur in the cruise mode from leaving exposed a system that can generate a section lift coefficient greater than 6.5 at $\alpha_g = 0$ deg in the high-lift mode. The supercritical airfoil thick contour can provide the already-proven favorable transonic cruise performance, and its thick leading edge provides a very effective nondeflecting anti-separation device to compliment the high circulation properties of the round trailing edge. The remaining unknown is the effect of the nonretracting small trailing edge on the drag characteristics of the airfoil in high subsonic and transonic flow. It is thus recommended that a transonic two-dimensional investigation be conducted to determine the unblown and low-blowing performance of the combined CCW/Supercritical configuration.

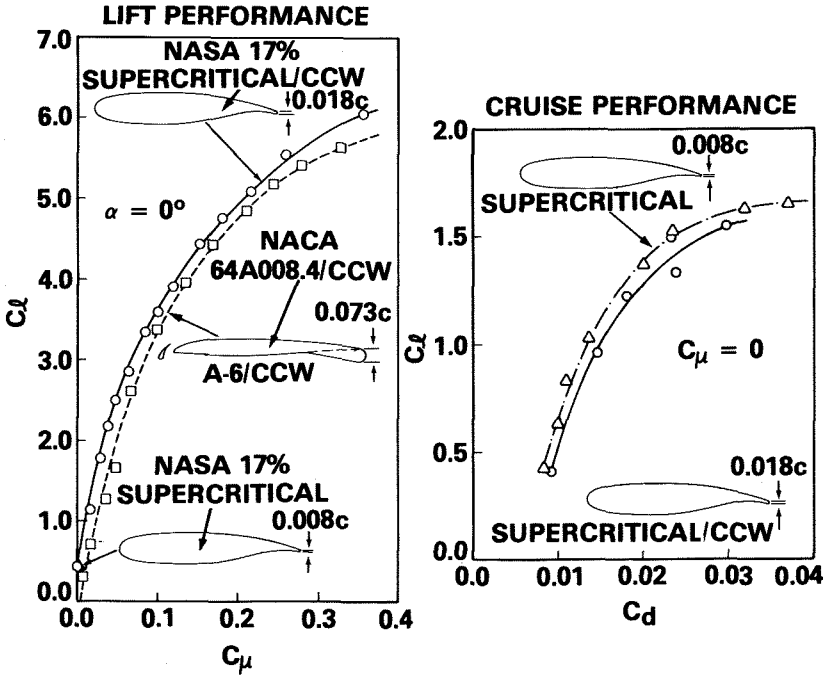

Fig. 22 - Small Trailing Edge CCW/Supercritical Airfoil Performance Comparisons

References

1. Englar, R.J., et al., "Design of the Circulation Control Wing STOL Demonstrator Aircraft," AIAA Paper No. 79-1842 presented at the AIAA Aircraft Systems and Technology Meeting, New York (Aug 1979). Republished in AIAA Journal of Aircraft, Vol. 18, No. 1, pp. 51-58 (Jan 1981).

2. Pugliese, A.J. and R.J. Englar, "Flight Testing the Circulation Control Wing," AIAA Paper No. 79-1791 presented at AIAA Aircraft Systems and Technology Meeting, New York (Aug 1979).

3. Englar, R.J., "Development of the A-6/Circulation Control Wing Flight Demonstrator Configuration," DTNSRDC Report ASED-79/01 (Jan 1979).

4. Englar, R.J., "Subsonic Two-Dimensional Wind Tunnel Investigations of the High Lift Capability of Circulation Control Wing Sections," DTNSRDC Report ASED-274 (Apr 1975).

5. Nichols, J.H., Jr., and R.J. Englar, "Advanced Circulation Control Wing System for Navy STOL Aircraft," AIAA Paper No. 80-1825 presented at the AIAA Aircraft Systems Meeting, Anaheim, California (4-6 Aug 1980).

6. Nichols, J.H., Jr., et al., "Experimental Development of an Advanced Circulation Control Wing System for Navy STOL Aircraft," AIAA Paper No. 81-0151 presented at the AIAA 19th Aerospace Sciences Meeting, St. Louis (12-15 Jan 1981).

7. McGhee, R.H. and G.H. Bingham, "Low-Speed Aerodynamic Characteristics of a 17-Percent Thick Supercritical Airfoil Section, Including a Comparison Between Wind-Tunnel and Flight Data," NASA TM X-2571 (Jul 1972).

8. Englar, R.J. and J. Ottensoser, "Calibration of Some Subsonic Wind Tunnel Inserts for Two-Dimensional Airfoil Experiments," DTNSRDC Report ASED AL-275 (Sept 1972).

9. Palmer, W.E., et al., "Flight and Wind-Tunnel Evaluation of a 17-Percent Thick Supercritical Airfoil on a T-2C Airplane," Vol. I and II, North American Rockwell Corp. Report NR71H-150 (Jul 1971).

10. Englar, R.J., "Experimental Investigation of the High Velocity Coanda Wall Jet Applied to Bluff Trailing Edge Circulation Control Airfoils," DTNSRDC Report 4708 (Sept 1975).

11. Englar, R.J., "Two-Dimensional Subsonic Wind Tunnel Test of a Cambered 30-Percent Thick Circulation Control Airfoil," DTNSRDC Report ASED AL-201 (May 1972).

12. Abbott, I.H. and A.E. Von Doenhoff, "Theory of Wing Sections," Dover Publications, New York (1959).

13. Alexander, A.J. and J. Williams, "Wind-Tunnel Experiments on a Rectangular-Wing Jet-Flap Model of Aspect-Ratio 6," ARC R&M No. 3329 (Jun 1961).

14. Ljungstrom, B.L.G., "Experimental High Lift Optimization of Multiple Element Airfoils," in AGARD Conference Proceedings No. 143 on V/STOL Aerodynamics (Apr 1974).

15. Harris, M.J., et al., "Development of the Circulation Control Wing/Upper Surface Blowing Powered-Lift System for STOL Aircraft," Paper ICAS-82-6.5.1 presented at the 13th ICAS/AIAA Aircraft Systems & Technology Conference, Seattle (22-27 Aug 1982).